Ion transport in glass: Influence of glassy structure on spatial extent of nonrandom ion hopping

B. Roling, C. Martiny, and S. Brückner
Institut für Physikalische Chemie, Westfälische Wilhelms-Universität Münster, and Sonderforschungsbereich 458, Schlossplatz 4/7, D-48149 Münster, Germany

(Received 17 April 2000; revised manuscript received 17 August 2000; published 1 May 2001)

On short time scales, the diffusion of mobile ions in glasses is nonrandom, i.e., the ions perform correlated forward-backward motions. By using linear response theory, we show in detail how typical distances characterizing the spatial extent of the nonrandom ionic diffusion can be derived from frequency-dependent conductivity data when the Haven ratio is known. We compare the dependence of these typical distances on the alkali content in germanate, borate, and silicate glasses. In all glasses, the typical distances decrease with increasing alkali oxide content. In the germanate and silicate glasses, the decrease is, however, more pronounced than in the borates. This network former effect points to the influence of the network structure on the spatial extent of the nonrandom diffusion.

DOI: 10.1103/PhysRevB.63.214203 PACS number(s): 66.30.Hs, 61.43.Fs, 66.30.Dn, 66.10.Ed

I. INTRODUCTION

Ion transport in glass is a thermally activated process. Therefore it is believed that the diffusion of the mobile ions occurs via hopping motions between well-defined potential minima in the glassy network. Information about these motions on different time and length scales can be obtained by using spectroscopic techniques, such as electrical conductivity spectroscopy, mechanical loss spectroscopy, and spin lattice relaxation spectroscopy.

For a given temperature T, the real part of the complex electrical conductivity of an ion conducting glass, $\sigma'(\nu)$, is independent of frequency and identical to the dc conductivity σ_{dc} when the frequency is lower than a characteristic frequency $\nu^*(T)$. $\nu^*(T)$ is thermally activated with the same activation energy as σ_{dc}. When the frequency exceeds $\nu^*(T)$, $\sigma'(\nu)$ increases with frequency. This dispersion indicates that on time scales shorter than $1/[2\pi\nu^*(T)]$, the ionic diffusion is nonrandom, i.e., the ions perform correlated forward-backward motions.[1–3] On the other hand, when the time window of the experiment is larger than $1/[2\pi\nu^*(T)]$, the ions behave like ''random walkers,'' i.e., the nonrandom motions on shorter time scales are not resolved anymore.

In the last decades, a large amount of frequency-dependent conductivity data of ion conducting glasses has been collected,[1,4–11] and many theoretical approaches have been developed in order to explain these data.[3,12–18] Nevertheless, a generally accepted theory of ion transport in glass does not yet exist. In our opinion, one important question that has not yet been answered satisfactorily is: What can be learned from frequency-dependent conductivity spectra about the role of (i) the disordered glassy network and (ii) the interionic interactions play for the ion dynamics? The disorder of the glassy network may lead to large fluctuations of the depth of potential minima and to large fluctuations of the heights of the potential barriers between the minima. It is well known that such static fluctuations can cause strong backward correlations in the ionic motions.[18–23] In several theoretical approaches, the importance of the interionic Coulomb interactions for the ion dynamics is emphasized.[1,15,24] As has been demonstrated by Maass and co-workers[2,3] and by Knödler *et al.*[25] with the help of Computer simulations, the combination of disorder and interionic interactions leads to an enhanced probability for correlated forward-backward hopping processes.

On the other hand, Dyre and co-workers have shown that the frequency-dependent conductivity of glasses can be reasonably well described by a single particle motion in a potential landscape with spatially uncorrelated random barriers.[18,19] i.e., it does not seem to be necessary to take into account the interactions between the particles to reproduce the experimentally observed characteristic shape of the conductivity spectra.

In a recent paper, we have shown that information on the spatial extent of the nonrandom ionic diffusion can be obtained from a combined analysis of frequency-dependent conductivity data and tracer diffusion data.[26] Such kind of information can be helpful to better assess the role of the network structure and of the interionic interactions. If the interionic Coulomb interactions were mainly responsible for the forward-backward motions, then one would expect that the spatial extent of the nonrandom diffusion is related to the interionic distances. On the other hand, if structural features were most important, one would expect correlations between the spatial extent of the nonrandom diffusion and structural peculiarities of the glasses.

We have found that in glasses with low concentrations of network modifying alkali oxides, the spatial extent of the nonrandom diffusion seems to be related to the interionic distances. On the other hand, in highly modified glasses, the dependence of the spatial extent on the alkali oxide content is different in different glassy systems based on different network formers. The latter observation clearly points to the influence of the glassy structure on the forward-backward motions of the mobile ions.

In this paper, we present a detailed theoretical derivation of typical distances characterizing the spatial extent of the nonrandom ion hopping. We explain in what way these typical distances can be calculated from experimental conductiv-

ity data when the Haven ratio is known. Furthermore, we present new experimental results on lithium borate glasses and on a sodium germanate glass. These results confirm that the composition dependence of the spatial extent of the nonrandom ion hopping is different in highly modified borate, germanate, and silicate glasses. We try to interprete these results in more detail than in Ref. 26 by taking into account the structural peculiarities of these glasses. It is well known that the structure of germanate glasses is characterized by the so-called ''germanate anomaly.'' [27–31] The structure of borate glasses exhibits a corresponding ''borate anomaly.'' [32,33] These anomalies seem to have a strong influence on the spatial extent of the nonrandom ion hopping in these glassy systems.

II. EXPERIMENT

Borate glasses of compositions $x\ Li_2O\cdot(1-x)\ B_2O_3$ with $x=0.128$, 0.226, and 0.333 and a germanate glass of composition $0.4\ Na_2O\cdot 0.6\,GeO_2$ were prepared by using the melt quenching technique. For the preparation of the borate glasses, Li_2CO_3 and B_2O_3 were dried at 170 °C for 1 day and then ground to fine powder using a mortar. The raw materials were melted in a platinum crucible at 1000 °C for 40 min and then cast onto a platinum plate.

For the preparation of the germanate glass, Na_2CO_3 and GeO_2 were dried in a platinum crucible at 500 °C for 30 min. In order to ensure a complete evaporation of carbon dioxide, the raw materials were held at 1000 °C for approximately 1 h. They were then melted at 1300 °C for 90 min. The melt was cast onto a platinum plate. This casting process was done in the furnace. Afterwards, the platinum plate was immediately removed from the furnace and cooled down to room temperature.

All glasses were annealed 30 K below their respective glass transition temperatures for 2 h and then cooled down to room temperature with a rate of 1 K/min. The surfaces of all samples were ground and polished, and metal electrodes were sputtered onto the sample surfaces. Frequency- and temperature-dependent conductivities $\hat{\sigma}(\nu,T)$ were measured using the LF impedance analyzer HP 4192 A.

III. RESULTS

It is well known that the conductivity spectra of glasses follow the time-temperature superposition principle, i.e., the conductivity isotherms of a given glass can be superimposed onto a master curve upon appropriate scaling of the conductivity and of the frequency axis.[6,7,10,11,34–36] A simple possibility to produce master curves of the real part of the conductivity without using arbitrary scaling parameters is to plot σ'/σ_{dc} vs $\nu/(\sigma_{dc}\cdot T)$.[11,36] In Fig. 1, we present such master curves for lithium borate glasses containing different amounts of lithium oxide. As seen from Fig. 1, the individual master curves are similar in shape. However, the master curves are shifted to higher values on the scaled frequency axis as the lithium oxide content x decreases. This has also been observed for sodium borate glasses of compositions x

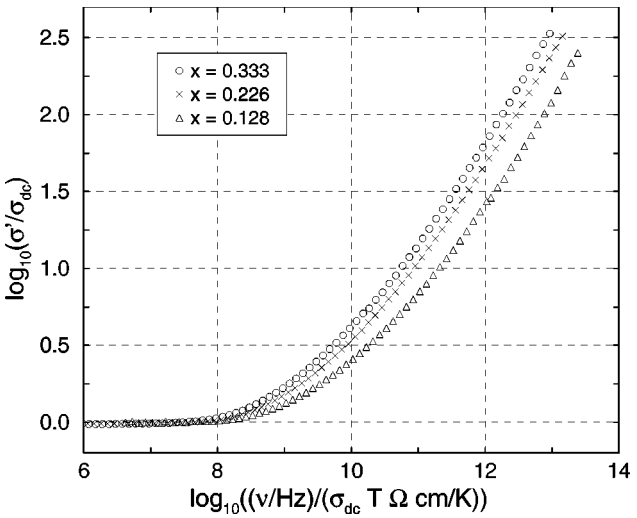

FIG. 1. Conductivity master curves of $x\ Li_2O\cdot(1-x)\ B_2O_3$ glasses.

$Na_2O\cdot(1-x)B_2O_3$ with $0.1\leqslant x\leqslant 0.3$. In that case, the position of the master curves on the $\nu/(\sigma_{dc}\cdot T)$ axis was found to scale with $1/x$.[36,37] In the case of the lithium borate glasses, the position of the master curves on the $\nu/(\sigma_{dc}\cdot T)$ axis does not exactly scale with $1/x$.

In Fig. 2, conductivity master curves for sodium germanate glasses of compositions $x\,Na_2O\cdot(1-x)GeO_2$ with $x=0.005$, 0.0099, 0.09, 0.213, and 0.40 are shown. As seen from the figure, the scaling behavior of these master curves is clearly distinct from that of the borate glasses. The master curves do not simply shift to higher values on the $\nu/(\sigma_{dc}\cdot T)$ axis as the sodium oxide content decreases, but the value of $\nu/(\sigma_{dc}\cdot T)$ where the conductivity becomes dispersive is minimal for the glass with $x=0.09$.

In the following sections we will show that the differences between the borate and the germanate glasses regarding the scaling behavior of the conductivity master curves

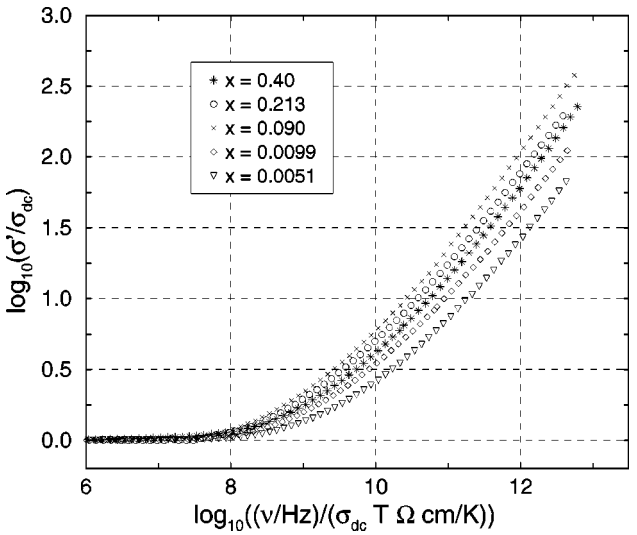

FIG. 2. Conductivity master curves of $x\ Na_2O\cdot(1-x)\ GeO_2$ glasses.

are related to different composition dependences of the spatial extent of the nonrandom ionic diffusion in these glasses.

IV. CALCULATION OF TYPICAL DISTANCES CHARACTERIZING THE SPATIAL EXTENT OF THE NONRANDOM IONIC DIFFUSION

A. Important functions and relations

- According to linear response theory, the frequency-dependent complex electrical conductivity $\hat{\sigma}(\nu)$ is proportional to the Fourier transform of the current density autocorrelation function $\langle \mathbf{J}(0)\cdot\mathbf{J}(t)\rangle$:[38]

$$\hat{\sigma}(\nu)=\frac{V}{3k_BT}\int_0^\infty \langle \mathbf{J}(0)\cdot\mathbf{J}(t)\rangle e^{-i2\pi\nu t}dt. \tag{1}$$

  Here, V is the volume of the sample, and k_B denotes Boltzmann's constant. In the following, we consider exclusively the contributions of ionic hops to the conductivity. In this case, we can relate the current density autocorrelation function to the charges q_i and the velocities $\mathbf{v}_i$ of the mobile ions:

$$\langle \mathbf{J}(0)\cdot\mathbf{J}(t)\rangle=\frac{1}{V^2}\left\langle \sum_{i,j}^{1\cdots N} q_i\mathbf{v}_i(0)\cdot q_j\mathbf{v}_j(t)\right\rangle. \tag{2}$$

Here, N is the number of mobile ions. In a material with only one mobile ionic species with charge q, the combination of Eqs. (1) and (2) results in

$$\hat{\sigma}(\nu)=\frac{q^2}{3Vk_BT}\int_0^\infty \left\langle \sum_{i,j}^{1\cdots N} \mathbf{v}_i(0)\cdot\mathbf{v}_j(t)\right\rangle e^{-i2\pi\nu t}dt. \tag{3}$$

$\langle \Sigma_{i,j}^{1\cdots N}\mathbf{v}_i(0)\cdot\mathbf{v}_j(t)\rangle$ is the velocity correlation function of the hopping ions.

- The frequency-dependent complex coefficient of self-diffusion of the mobile ions is proportional to the Fourier transform of the velocity autocorrelation function of the mobile ions $\langle \mathbf{v}(0)\cdot\mathbf{v}(t)\rangle$:[39]

$$\hat{D}(\nu)=\frac{1}{3}\int_0^\infty \langle \mathbf{v}(0)\cdot\mathbf{v}(t)\rangle e^{-i2\pi\nu t}dt. \tag{4}$$

- Electrical conductivity and coefficient of self-diffusion may be related via a generalized Nernst-Einstein equation:[3]

$$\hat{\sigma}(\nu)=\frac{N_V q^2}{k_BT}\frac{1}{\hat{H}_R(\nu)}\hat{D}(\nu) \tag{5}$$

$$\text{with}\quad \hat{H}_R(\nu\to 0)=H_R.$$

  Here, N_V is the number density of the mobile ions, while $\hat{H}_R(\nu)$ denotes a frequency-dependent complex Haven ratio.[3] The low-frequency limit of the complex Haven ratio H_R can be obtained from measurement of the dc conductivity $\sigma_{\rm dc}$ and of the low-frequency limit of the coefficient of self-diffusion $D=\hat{D}(\nu\to 0)$. Often, D is obtained by using radio tracer techniques.

- When correlations between the velocities of different ions can be neglected, the velocity correlation function is proportional to the velocity autocorrelation function.[1]

$$\left\langle \sum_{i,j}^{1\cdots N} \mathbf{v}_i(0)\cdot\mathbf{v}_j(t)\right\rangle = N\langle \mathbf{v}(0)\cdot\mathbf{v}(t)\rangle. \tag{6}$$

  In this case, the Haven ratio is frequency independent and unity. When cross correlations cannot be neglected, the Haven ratio is a complex function of the frequency.[3]
- Furthermore, we will use the following functions:

(i) the velocity-space correlation functions

$$\left\langle \sum_{i,j}^{1\cdots N} \mathbf{v}_i(0)\cdot\mathbf{r}_j(t)\right\rangle = \int_0^t \left\langle \sum_{i,j}^{1\cdots N} \mathbf{v}_i(0)\cdot\mathbf{v}_j(t')\right\rangle dt' \tag{7}$$

and

$$\langle \mathbf{v}(0)\cdot\mathbf{r}(t)\rangle=\int_0^t \langle \mathbf{v}(0)\cdot\mathbf{v}(t')\rangle dt', \tag{8}$$

(ii) the mean-square displacement of the mobile ions:

$$\begin{aligned}\langle r^2(t)\rangle&=\frac{1}{N}\left\langle \sum_{i=1}^{N}\Delta\mathbf{r}_i^2(t)\right\rangle\\ &=2\int_0^t\langle \mathbf{v}(0)\cdot\mathbf{r}(t')\rangle dt'\\ &=2\int_0^t\int_0^{t'}\langle \mathbf{v}(0)\cdot\mathbf{v}(t'')\rangle dt''dt',\end{aligned} \tag{9}$$

(iii) the function $\langle R^2(t)\rangle$ which is proportional to the mean-square displacement of the center of charge of the mobile ions:

$$\begin{aligned}\langle R^2(t)\rangle&=\frac{1}{N}\left\langle\left(\sum_{i=1}^{N}\Delta\mathbf{r}_i(t)\right)^2\right\rangle\\ &=\frac{2}{N}\int_0^t\left\langle \sum_{i,j}^{1\cdots N}\mathbf{v}_i(0)\cdot\mathbf{r}_j(t')\right\rangle dt'\\ &=\frac{2}{N}\int_0^t\int_0^{t'}\left\langle \sum_{i,j}^{1\cdots N}\mathbf{v}_i(0)\cdot\mathbf{v}_j(t'')\right\rangle dt''dt',\end{aligned} \tag{10}$$

(iv) the conductivity diffusion coefficient of the mobile ions:

$$\begin{aligned}\hat{D}_\sigma(\nu)&=\hat{\sigma}(\nu)\frac{k_BT}{N_Vq^2}\\ &=\frac{1}{3N}\int_0^\infty\left\langle \sum_{i,j}^{1\cdots N}\mathbf{v}_i(0)\cdot\mathbf{v}_j(t)\right\rangle e^{-i2\pi\nu t}dt,\end{aligned} \tag{11}$$

(v) and the frequency-dependent complex dielectric function:

$$\hat{\epsilon}(\nu)=[\hat{\sigma}(\nu)-\sigma_{\rm dc}]/(i2\pi\nu\epsilon_0). \tag{12}$$

Here, ϵ_0 is the permittivity of free space.

- In the following, the symmetry of different correlation functions will play an important role:

$\langle \Sigma_{i,j}^{1\cdots N} \mathbf{v}_i(0)\cdot\mathbf{v}_j(t)\rangle$ and $\langle \mathbf{v}(0)\cdot\mathbf{v}(t)\rangle$ are even functions of time,
$\langle \Sigma_{i,j}^{1\cdots N} \mathbf{v}_i(0)\cdot\mathbf{r}_j(t)\rangle$ and $\langle \mathbf{v}(0)\cdot\mathbf{r}(t)\rangle$ are odd functions of time,
$D'(\nu)$ and $D'_\sigma(\nu)$ are even functions of frequency,
$D''(\nu)$ and $D''_\sigma(\nu)$ are odd functions of frequency.

B. Calculation of a characteristic distance $\sqrt{\langle r^2(t_p)\rangle}$ from the real and the imaginary part of the conductivity

From Eq. (4) it follows for the real part of the complex coefficient of self-diffusion:

$$D'(\nu)=\frac{1}{3}\int_0^\infty \langle \mathbf{v}(0)\cdot\mathbf{v}(t)\rangle \cos(2\pi\nu t)dt. \tag{13}$$

Since $\langle \mathbf{v}(0)\cdot\mathbf{v}(t)\rangle$ is an even function of time, we may write

$$D'(\nu)=\frac{1}{6}\int_{-\infty}^\infty \langle \mathbf{v}(0)\cdot\mathbf{v}(t)\rangle e^{-i2\pi\nu t}dt. \tag{14}$$

When we now perform an inverse Fourier transformation, we obtain the following expression for the velocity autocorrelation function:

$$\langle \mathbf{v}(0)\cdot\mathbf{v}(t)\rangle = 6\int_{-\infty}^\infty D'(\nu)e^{i2\pi\nu t}d\nu. \tag{15}$$

Integration of this equation in the limits from 0 to t results in (see the Appendix, Sec. 1):

$$\begin{aligned}\langle \mathbf{v}(0)\cdot\mathbf{r}(t)\rangle &= \int_0^t \langle \mathbf{v}(0)\cdot\mathbf{v}(t')\rangle dt' \\ &= 6\int_{-\infty}^\infty \frac{D'(\nu)}{i2\pi\nu}(e^{i2\pi\nu t}-1)d\nu \\ &= 6\left(\int_{-\infty}^\infty \frac{D'(\nu)}{i2\pi\nu}e^{i2\pi\nu t}d\nu - \int_{-\infty}^\infty \frac{D'(\nu)}{i2\pi\nu}d\nu\right).\end{aligned} \tag{16}$$

Since $D'(\nu)/\nu$ is an odd function of frequency, the second term in the brackets is zero. It follows for the velocity space correlation function:

$$\begin{aligned}\langle \mathbf{v}(0)\cdot\mathbf{r}(t)\rangle &= \frac{6}{2\pi}\int_{-\infty}^\infty \frac{D'(\nu)}{\nu}\sin(2\pi\nu t)d\nu \\ &= \frac{6}{\pi}\int_0^\infty \frac{D'(\nu)}{\nu}\sin(2\pi\nu t)d\nu.\end{aligned} \tag{17}$$

Integration in the limits from 0 to t and multiplication by a factor of 2 on both sides of this equation results in the following expression for the mean-square displacement of the mobile ions:

$$\langle r^2(t)\rangle = \frac{12}{\pi}\int_0^t dt'\int_0^\infty \frac{D'(\nu)}{\nu}\sin(2\pi\nu t')d\nu. \tag{18}$$

With the Nernst-Einstein Eq. (5) we may write

$$\langle r^2(t)\rangle = \frac{12k_BT}{N_Vq^2\pi}\int_0^t dt'\int_0^\infty \frac{\mathrm{Re}[\hat\sigma(\nu)\hat H_R(\nu)]}{\nu}\sin(2\pi\nu t')d\nu. \tag{19}$$

Here, Re denotes the real part of a complex function.

For ion conducting glasses with low alkali oxide contents (1 mol % and below), the low-frequency limiting value of the complex Haven ratio H_R is close to unity.[40–42] In highly modified glasses, H_R is usually around 0.3.[40,42,43] In the limit of high frequencies, $\hat H_R(\nu)$ is expected to approach unity, independent of the ionic concentrations. This is because on very short time scales the ionic hops should be independent.[1,3] Therefore $\hat H_R(\nu)$ should be a weak function of frequency. The real part of the Haven ratio, $H'_R(\nu)$, should increase from H_R at frequencies below the onset frequency of the conductivity dispersion to unity at high frequencies. Maass *et al.* have shown with the help of Monte Carlo simulations that this is, indeed, the case for the hopping motions of interacting particles in disordered potential landscapes.[3]

In the case of our low-frequency conductivity spectra, $\hat H_R(\nu)\approx H_R$ should therefore be a good approximation. The mean-square displacement of the mobile ions can then be approximated by

$$\langle r^2(t)\rangle = \frac{12k_BT\,H_R}{N_Vq^2\pi}\int_0^t dt'\int_0^\infty \frac{\sigma'(\nu)}{\nu}\sin(2\pi\nu t')d\nu. \tag{20}$$

This equation is used to calculate $\langle r^2(t)\rangle$ curves for our glasses. Values for H_R are taken from the literature.[40,42,43] The temperature dependence of these values is neglected, since it has been found that the temperature dependence of the Haven ratio is usually very small. Some authors observed that H_R increases slightly with temperature,[44–46] while other authors found no consistent trend with temperature.[47,48] Even if our glasses showed a slight increase of H_R with temperature, this would not qualitatively affect our results for the composition dependence of the spatial extent of the nonrandom ion hopping.

In Fig. 3 we present exemplarily a master curve of the mean-square displacement of the lithium ions, $\langle r^2(t)\rangle$, in a 0.333 $Li_2O\cdot 0.667\ B_2O_3$ glass. Note that this mean-square displacement is exclusively due to hopping motions of the lithium ions. As seen from the figure, $\langle r^2\rangle$ is a function of $t\cdot\sigma_{dc}\cdot T$, independent of temperature. This implies that the position of the mean-square displacement curves on the time scale depends on temperature, while the value of $\langle r^2\rangle$ at characteristic points of the curves is independent of temperature. In the limit of long times, $\langle r^2(t)\rangle$ is proportional to time, while at short times the diffusion is nonrandom, i.e., the mean-square displacement depends on time in a sublinear fashion. From the scaling properties of the mean-square displacement curves, it follows that the typical value of $\langle r^2(t)\rangle$

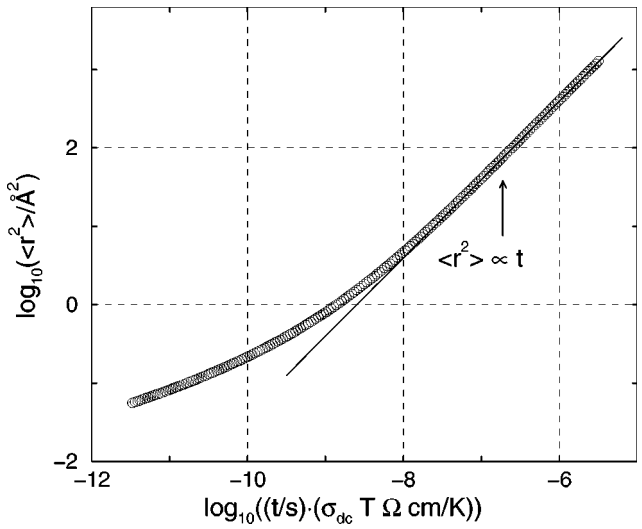

FIG. 3. Master curve of the mean-square displacement of the lithium ions in a 0.333 $Li_2O \cdot 0.667\ B_2O_3$ glass.

where the nonrandom diffusion passes over into a random diffusion does not depend on temperature. The only problem is to define one characteristic crossover point and thus one characteristic value of the mean-square displacement.

We suggest the following. For ion conducting glasses, the imaginary part of the dielectric function, with $\hat{\varepsilon}(\nu)$ as defined in Eq. (12), exhibits a peak. The peak frequency ν_p is in the crossover range from the dc conductivity to the dispersive conductivity. This is shown exemplarily in Fig. 4 for a 0.333 $Li_2O \cdot 0.667\ B_2O_3$ glass. Note that we did not calculate $\varepsilon''(\nu)$ from the real part of the conductivity after subtraction of the dc conductivity but by a Kramers-Kronig transformation of $\varepsilon'(\nu)$. This procedure avoids large errors due to the subtraction of similar numbers. Now, we calculate the mean-square displacement of the mobile ions at the characteristic time $t_p = 1/(2 \cdot \pi \cdot \nu_p)$. The square root of this value, $\sqrt{\langle r^2(t_p)\rangle}$, is taken as a distance characterizing the crossover from nonrandom diffusion to random diffusion.

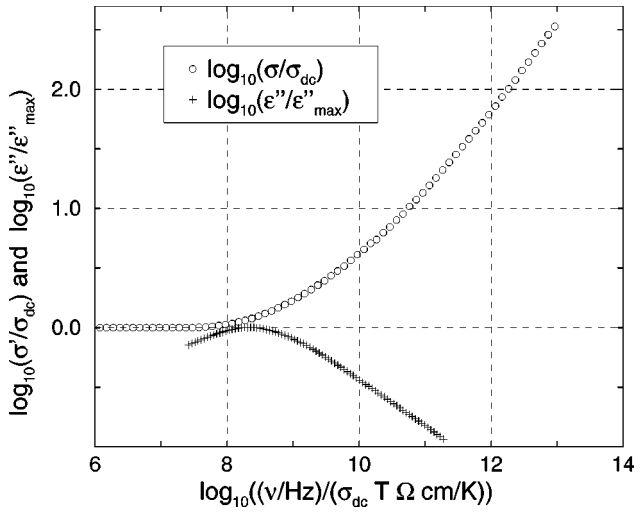

FIG. 4. Conductivity and dielectric loss master curves for a 0.333 $Li_2O \cdot 0.667\ B_2O_3$ glass.

C. Calculation of a characteristic distance $\sqrt{\langle \tilde{R}^2(\infty)\rangle}$ from the imaginary part of the conductivity

From Eq. (11) it follows for the imaginary part of the conductivity diffusion coefficient:

$$D''_\sigma(\nu) = -\frac{1}{3N}\int_0^\infty \left\langle \sum_{i,j}^{1\cdots N} \mathbf{v}_i(0)\cdot\mathbf{v}_j(t)\right\rangle \sin(2\pi\nu t)dt. \tag{21}$$

Using the function

$$\begin{aligned} A(t) &= 1 \quad \text{for} \quad t>0, \\ &= 0 \quad \text{for} \quad t=0, \\ &= -1 \quad \text{for} \quad t<0, \end{aligned} \tag{22}$$

we may write for the conductivity diffusion coefficient

$$\begin{aligned} D''_\sigma(\nu) &= -\frac{1}{6N}\int_{-\infty}^\infty \left\langle \sum_{i,j}^{1\cdots N} \mathbf{v}_i(0)\cdot\mathbf{v}_j(t)\right\rangle A(t)\sin(2\pi\nu t)dt \\ &= \frac{1}{6Ni}\int_{-\infty}^\infty \left\langle \sum_{i,j}^{1\cdots N} \mathbf{v}_i(0)\cdot\mathbf{v}_j(t)\right\rangle A(t)e^{-i2\pi\nu t}dt. \end{aligned} \tag{23}$$

An inverse Fourier transformation results in

$$\left\langle \sum_{i,j}^{1\cdots N} \mathbf{v}_i(0)\cdot\mathbf{v}_j(t)\right\rangle A(t) = 6Ni\int_{-\infty}^\infty D''_\sigma(\nu)e^{i2\pi\nu t}d\nu. \tag{24}$$

When we integrate this equation in the limits from 0 bis t, we obtain (see the Appendix, Sec. 1):

$$\begin{aligned} &\int_0^t \left\langle \sum_{i,j}^{1\cdots N} \mathbf{v}_i(0)\cdot\mathbf{v}_j(t')\right\rangle A(t')dt' \\ &\quad = 6Ni\int_{-\infty}^\infty \frac{D''_\sigma(\nu)}{i2\pi\nu}(\epsilon^{i2\pi\nu t}-1)d\nu. \end{aligned} \tag{25}$$

Therefore

$$\begin{aligned} \left\langle \sum_{i,j}^{1\cdots N} \mathbf{v}_i(0)\cdot\mathbf{r}_j(t)\right\rangle &= 6N\int_{-\infty}^\infty \frac{D''_\sigma(\nu)}{2\pi\nu}e^{i2\pi\nu t}d\nu \\ &\quad - 6N\int_{-\infty}^\infty \frac{D''_\sigma(\nu)}{2\pi\nu}d\nu. \end{aligned} \tag{26}$$

As shown in the Appendix, Sec. 2, the second term on the right-hand side of the equation is equal to $-3ND'_\sigma(0)$. Thus we obtain

$$\left\langle \sum_{i,j}^{1\cdots N} \mathbf{v}_i(0)\cdot(0)\cdot\mathbf{r}_j(t)\right\rangle - 3ND'_\sigma(0) = \frac{6N}{\pi}\int_0^\infty \frac{D''_\sigma(\nu)}{\nu}\cos(2\pi\nu t)d\nu. \quad (27)$$

Integration of this equation in the limits from 0 bis t and multiplication by a factor of $2/N$ results in the following expression for $\langle R^2(t)\rangle$:

$$\langle R^2(t)\rangle - 6D'_\sigma(0)t = \frac{12}{\pi}\int_0^t dt' \int_0^\infty \frac{D''_\sigma(\nu)}{\nu}\cos(2\pi\nu t')d\nu. \quad (28)$$

In the following, we replace $\langle R^2(t)\rangle - 6D'_\sigma(0)t$ by $\langle \tilde{R}^2(t)\rangle$. Taking into account Eq. (11) we may write

$$\langle \tilde{R}^2(t)\rangle = \frac{12k_BT}{N_V q^2\pi}\int_0^t dt' \int_0^\infty \frac{\sigma''(\nu)}{\nu}\cos(2\pi\nu t')d\nu. \quad (29)$$

When we finally replace the imaginary part of the conductivity by the real part of the dielectric function [see Eq. (12)], we arrive at

$$\langle \tilde{R}^2(t)\rangle = \frac{24k_BT\epsilon_0}{N_V q^2}\int_0^t dt' \int_0^\infty [\epsilon'(\nu)-\epsilon'(\infty)] \times\cos(2\pi\nu t')d\nu. \quad (30)$$

In this equation, the high-frequency limiting value $\epsilon'(\infty)$ was subtracted from the dielectric function because this value is due to vibrational and electronic polarizations.

In ion conducting glasses, the dielectric function approaches a limiting value, $\epsilon'(0)$, in the limit of low frequencies. Accordingly, the long-time limiting value of the function $\langle \tilde{R}^2(t)\rangle$ is given by

$$\langle \tilde{R}^2(\infty)\rangle = \frac{6k_BT\epsilon_0}{N_V q^2}[\epsilon'(0)-\epsilon'(\infty)]. \quad (31)$$

It would also be interesting to derive the corresponding single-particle quantity

$$\langle \tilde{r}^2(\infty)\rangle = \lim_{t\to\infty}\langle r^2(t)\rangle - 6D'(0)t. \quad (32)$$

To this end, we have to replace $D''_\sigma(\nu)$ by $D''(\nu)$ on the right-hand side of Eq. (28). From this it follows that

$$\langle \tilde{r}^2(\infty)\rangle = \frac{3}{\pi}\lim_{\nu\to 0}\frac{D''(\nu)}{\nu}. \quad (33)$$

Thus in order to calculate $\langle \tilde{r}^2(\infty)\rangle$, one needs information on the frequency dependence of the imaginary part of the Haven ratio, $H''_R(\nu)$, which is not accessible experimentally. Only at very low ionic concentrations where $H_R \approx 1$, $H''_R(\nu)$ should be close to zero for all frequencies, so that $\langle \tilde{r}^2(\infty)\rangle$ should be virtually identical to $\langle \tilde{R}^2(\infty)\rangle$. In the following, we show exclusively results for the many particle quantity $\langle \tilde{R}^2(\infty)\rangle$ which was calculated by using Eq. (31).

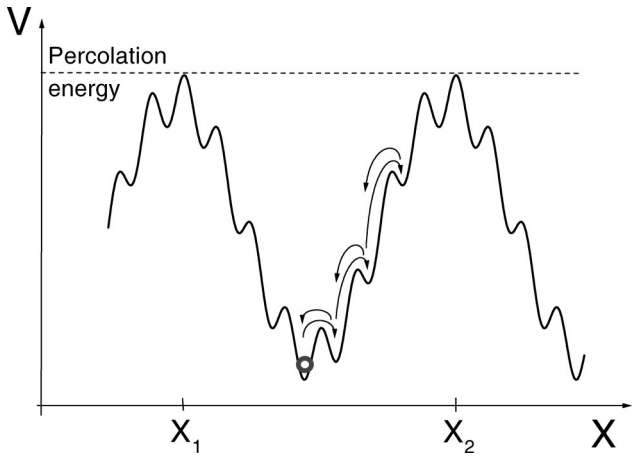

FIG. 5. Illustration of correlated forward-backward hops in a simple potential landscape.

V. DISCUSSION

Before we present results for the composition dependence of the characteristic distances $\sqrt{\langle r^2(t_p)\rangle}$ and $\sqrt{\langle \tilde{R}^2(\infty)\rangle}$ in our glasses, we would first like to discuss the physical meaning of these quantities. As seen from Fig. 4 the dielectric loss peak frequency ν_p occurs in the crossover regime from the dc to the dispersive conductivity. This means that in the corresponding time window of the order of $t_p = 1/(2\pi\nu_p)$, the nonrandom ionic diffusion passes over into a random diffusion. Therefore we can consider $\sqrt{\langle r^2(t_p)\rangle}$ as a typical distance the mobile ions have to cover to overcome the backward-driving forces causing the correlated forward-backward motions of the mobile ions. This is illustrated schematically in Fig. 5 for an ion moving in a potential landscape where the potential energy of the ion differs from site to site. The figure shows a one-dimensional illustration, but let us imagine the ion moves in a three-dimensional landscape. Of course, the ion will prefer to be on low-energy sites. When the ion now performs a hop to a higher-energy site, the probability for a backward jump will be higher than the probability for jumps into other directions simply because of the small barrier for the backward jump. That means that on short time scales, the ion dynamics will be characterized by correlated forward-backward hops. In order to perform a long-range diffusion, the ion has to overcome the percolation barriers. These are the highest barriers on percolation paths through the system. When the time becomes longer than the average time required for hopping processes over the percolation barriers, the ion is able to move between low-energy sites separated by the percolation barriers. On these time scales, the ion behaves like a random walker, i.e., the ion seems to move randomly from one low-energy site to the next, and the forward-backward hops on short time scales are not resolved anymore. Consequently, the characteristic distance $\sqrt{\langle r^2(t_p)\rangle}$ should be roughly the average distance the ion has to cover to overcome one of the nearest percolation barriers.

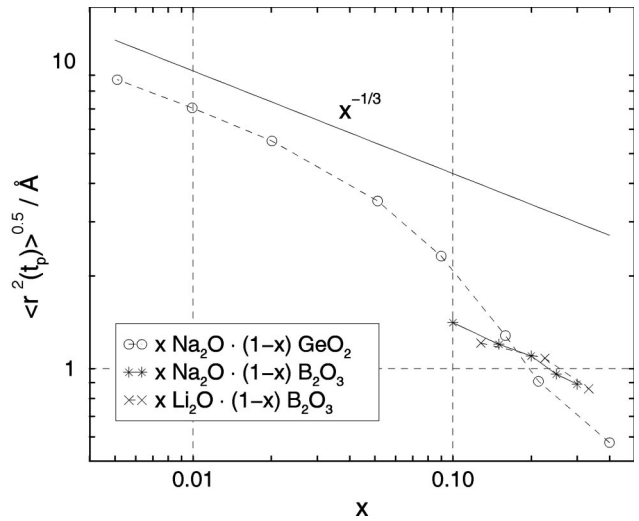

FIG. 6. Plot of the characteristic length $\sqrt{\langle r^2(t_p)\rangle}$ for sodium germanate, lithium borate, and sodium borate glasses.

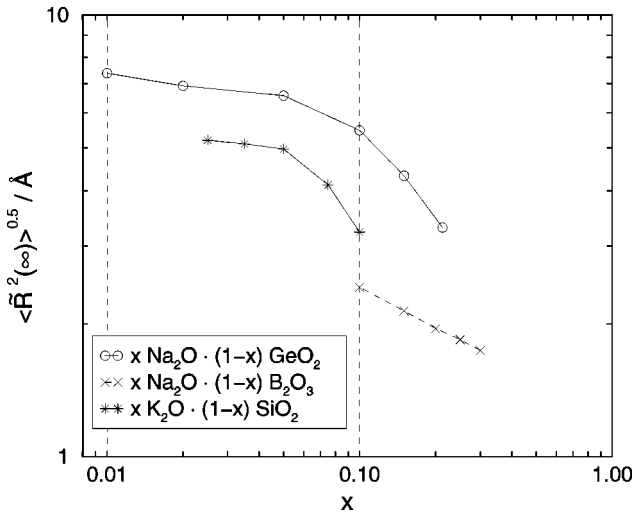

FIG. 7. Plot of the characteristic length $\sqrt{\langle \tilde{R}^2(\infty)\rangle}$ for sodium germanate, sodium borate, and potassium silicate glasses.

Note that there will be no generally valid relation between the distance $\sqrt{\langle r^2(t_p)\rangle}$ and the elementary hopping distance between two neighboring sites *a*. For a given value of *a*, the distance $\sqrt{\langle r^2(t_p)\rangle}$ will depend on the shape of the potential landscape, e.g., on the degree of spatial correlations between the site energies and between the barrier heights.

Let us now imagine that we ''switch off'' the long-range ionic diffusion by introducing periodic boundary conditions at the percolation barriers. When the ion overcomes one of the percolation barriers and moves into a neighboring ''valley,'' we put it back into the original ''valley.'' In this case, we observe exclusively forward-backward hops of the mobile ion. Therefore the introduction of periodic boundary conditions corresponds to the substraction of $6Dt$ from the mean-square displacement of the ion, $\langle r^2(t)\rangle$. In other words, the function $\langle \tilde{r}^2(t)\rangle = \langle r^2(t)\rangle - 6Dt$ describes the forward-backward hops in regions limited by the percolation barriers. Since this is a localized kind of motion, $\langle \tilde{r}^2(t)\rangle$ tends towards a limiting value $\langle \tilde{r}^2(\infty)\rangle$ in the limit of long times. This limiting value characterizes the spatial extent of the localized motions.

It is important to realize that also the relation between the distance $\sqrt{\langle \tilde{r}^2(\infty)\rangle}$ and the elementary hopping distance *a* depends on the shape of the potential landscape. Note that $\sqrt{\langle \tilde{r}^2(\infty)\rangle}$ can be even smaller than *a*. This is the case, if the site energies in the valleys differ enormously, so that the ion mainly occupies the lowest-energy site and stays only for very short time intervals on sites with higher energies.

Experimentally, one cannot determine $\sqrt{\langle \tilde{r}^2(\infty)\rangle}$ but only the many particle quantity $\sqrt{\langle \tilde{R}^2(\infty)\rangle}$. For the calculation of $\sqrt{\langle \tilde{R}^2(\infty)\rangle}$ in a model potential landscape, one has to additionally take into account cross correlations between the movements of different ions.

In Fig. 6 the composition dependence of the characteristic distance $\sqrt{\langle r^2(t_p)\rangle}$ is shown for sodium germanate, lithium borate, and sodium borate glasses. For all glasses, $\sqrt{\langle r^2(t_p)\rangle}$ decreases with increasing alkali oxide content. In the case of the sodium germanate glass containing 0.5 mol % Na_2O, we find that $\sqrt{\langle r^2(t_p)\rangle} = 8.7$ Å. For the highly modified germanate and borate glasses, $\sqrt{\langle r^2(t_p)\rangle}$ is around 1 Å or even smaller.

In the case of the germanate glasses with low sodium oxide contents, $\sqrt{\langle r^2(t_p)\rangle}$ is roughly proportional to $x^{-1/3}$. At sodium oxide contents $x \geqslant 0.15$, $\sqrt{\langle r^2(t_p)\rangle}$ decreases much faster with increasing *x*. By way of contrast, in the case of the highly modified borate glasses with $0.10 \leqslant x \leqslant 0.333$, $\sqrt{\langle r^2(t_p)\rangle}$ decreases roughly with $x^{-1/3}$. Note that the values of $\sqrt{\langle r^2(t_p)\rangle}$ for the lithium borate glasses and for the sodium borate glasses are very similar.

In Fig. 7 the characteristic distance $\sqrt{\langle \tilde{R}^2(\infty)\rangle}$ is plotted versus the alkali oxide content for sodium germanate, sodium borate, and potassium silicate glasses. Values for the dielectric relaxation strength $\epsilon'(0) - \epsilon'(\infty)$ of the potassium silicate glasses were taken from Ref. 49. In the case of the 0.005 $Na_2O \cdot 0.995$ GeO_2 glass, the 0.4 $Na_2O \cdot 0.6$ GeO_2 glass, and the lithium borate glasses, the characteristic distance $\sqrt{\langle \tilde{R}^2(\infty)\rangle}$ could not be calculated. The reason is that owing to electrode polarization effects, an $\epsilon'(0)$ plateau was not detected. As seen from the figure, the composition dependence of $\sqrt{\langle \tilde{R}^2(\infty)\rangle}$ is similar to that of $\sqrt{\langle r^2(t_p)\rangle}$. At alkali oxide contents above a few mol %, the composition dependence of $\sqrt{\langle \tilde{R}^2(\infty)\rangle}$ clearly depends on the nature of the network former. For the germanate and silicate glasses, $\sqrt{\langle \tilde{R}^2(\infty)\rangle}$ decays much faster with increasing *x* than for the borate glasses. This network former effect points to the influence of the glassy structure on the spatial extent of the nonrandom ionic diffusion.

In order to see whether there are correlations between the composition dependence of $\sqrt{\langle r^2(t_p)\rangle}$ and $\sqrt{\langle \tilde{R}^2(\infty)\rangle}$ and structural peculiarities of the glasses, let us now consider in what way the addition of alkali oxide changes the network structure of borate, germanate, and silicate glasses.

Glassy B_2O_3 consists of trigonal BO_3 units. A part of these units forms boroxol rings.[50–52] On the addition of alkali

oxides trigonally coordinated boron is converted into tetrahedrally coordinated boron. The degree of polymerization of the network is thereby enhanced, and a variety of different structural units (diborate, tetraborate, etc.) is produced.[32] When the alkali oxide content exceeds about 25–30 mol %, B–O–B bonds are broken and nonbridging oxygens are formed,[33] i.e., the network depolymerizes with increasing alkali oxide content. The maximum alkali oxide content of the glasses studied here is 33.3 mol %. Therefore even our highly modified borate glasses are highly polymerized and contain no or only few nonbridging oxygens.

Glassy GeO_2 consists of GeO_4 tetrahedra. At modifier contents below 15 mol %, the addition of a network modifier leads mainly to a conversion of GeO_4 tetrahedra into GeO_6 octahedra and thereby to an enhanced degree of polymerization.[27–31] When more than 15 mol % modifier is added, nonbridging oxygens are formed and the network depolymerizes with increasing modifier content.

Glassy SiO_2 consists of SiO_4 tetrahedra. The addition of alkali oxide always leads to a breaking of S–O–Si bonds and to the formation of nonbridging oxygens.[53–55]

These structural features suggest that the depolymerization of the network due to the formation of nonbridging oxygens plays an important role for the spatial extent of the nonrandom ionic diffusion. In the highly polymerized borate glasses containing no or only few nonbridging oxygens, the characteristic distances $\sqrt{\langle r^2(t_p)\rangle}$ and $\sqrt{\langle \tilde{R}^2(\infty)\rangle}$ are roughly proportional to $x^{-1/3}$. A similar composition dependence is observed for the germanate glasses with $x<0.15$ which do not contain nonbridging oxygens. At alkali oxide contents above 15 mol %, the network depolymerizes due to the formation of nonbridging oxygens, and we observe that $\sqrt{\langle r^2(t_p)\rangle}$ and $\sqrt{\langle \tilde{R}^2(\infty)\rangle}$ decrease much faster than with $x^{-1/3}$. In the case of the potassium silicate glasses where the addition of alkali oxide always leads to the formation of nonbridging oxygens, the fast decay of $\sqrt{\langle \tilde{R}^2(\infty)\rangle}$ with increasing x is already observed at very low alkali oxide contents.

In order to check whether the spatial extent of the nonrandom ion hopping and the degree of depolymerization of the glassy network are generally correlated, we plan further experimental studies. In particular, studies on aluminosilicate glasses seem to be promising. In these glasses, the amount of nonbridging oxygens can be varied at constant alkali oxide content by varying the ratio of the Al_2O_3 content to the SiO_2 content.

VI. SUMMARY

From the electrical conductivity spectra of ion conducting glasses, we have derived the characteristic distances $\sqrt{\langle r^2(t_p)\rangle}$ and $\sqrt{\langle \tilde{R}^2(\infty)\rangle}$, which contain information on the spatial extent of the nonrandom ion hopping. The composition dependences of $\sqrt{\langle r^2(t_p)\rangle}$ and $\sqrt{\langle \tilde{R}^2(\infty)\rangle}$ have been analyzed for sodium germanate, sodium borate, lithium borate and potassium silicate glasses. We find that $\sqrt{\langle r^2(t_p)\rangle}$ and $\sqrt{\langle \tilde{R}^2(\infty)\rangle}$ decrease with increasing alkali oxide content. However, the decrease is clearly more pronounced in the germanate and silicate glasses as compared to the borates. This network former effect points to the influence of the network structure on the microscopic dynamics of the mobile ions. The analysis of our results in relation to the structural peculiarities of the glasses suggests that the depolymerization of the network due to the formation of nonbridging oxygens leads to a strong decrease of the spatial extent of the nonrandom ion hopping. Further experimental studies will be performed to test this hypothesis.

ACKNOWLEDGMENTS

We are grateful to J. C. Dyre, K. Funke, A. Heuer, and D. L. Sidebottom for many helpful discussions. This work was supported by the Deutsche Forschungs-gemeinschaft in the framework of the Sonderforschungsbereich 458.

APPENDIX

1.

Consider the following pair of Fourier transforms:

$$f(t)=\int_{-\infty}^{\infty}\hat{F}(\nu)e^{i2\pi\nu t}d\nu. \tag{A1}$$

Integration of $f(t)$ in the limits from t_1 to t_2 results in

$$\begin{aligned}\int_{t_1}^{t_2}f(t)dt&=\int_{t_1}^{t_2}dt\int_{-\infty}^{\infty}\hat{F}(\nu)e^{i2\pi\nu t}d\nu\\&=\int_{-\infty}^{\infty}\left(\int_{t_1}^{t_2}e^{i2\pi\nu t}dt\right)\hat{F}(\nu)d\nu\\&=\int_{-\infty}^{\infty}\frac{\hat{F}(\nu)}{i2\pi\nu}(e^{i2\pi\nu t_2}-e^{i2\pi\nu t_1})d\nu.\end{aligned} \tag{A2}$$

2.

Consider the integral I which is given by

$$I=6N\int_{-\infty}^{\infty}\frac{D''_\sigma(\nu)}{2\pi\nu}d\nu. \tag{A3}$$

Taking into account Eq. (21) we obtain

$$\begin{aligned}I&=\frac{6N}{2\pi}\int_{-\infty}^{\infty}d\nu\frac{1}{\nu}\cdot\left(-\frac{1}{3\cdot N}\right)\\&\quad\times\int_0^{\infty}\left\langle\sum_{i,j}^{l\cdots N}\mathbf{v}_i(0)\cdot\mathbf{v}_j(t)\right\rangle\sin(2\pi\nu t)dt)dt\\&=-\frac{1}{\pi}\cdot\int_0^{\infty}\left\langle\sum_{i,j}^{l\cdots N}\mathbf{v}_i(0)\cdot\mathbf{v}_j(t)\right\rangle\left(\int_{-\infty}^{\infty}d\nu\frac{1}{\nu}\sin(2\pi\nu t)\right)dt.\end{aligned} \tag{A4}$$

The integral in the brackets is equal to π. Taking into account Eq. (11) we arrive at

$$I=-3ND'_\sigma(0). \tag{A5}$$

[1] K. Funke, Prog. Solid State Chem. **22**, 111 (1993).
[2] P. Maass, J. Petersen, A. Bunde, W. Dieterich, and H. E. Roman, Phys. Rev. Lett. **66**, 52 (1991).
[3] P. Maass, M. Meyer, and A. Bunde, Phys. Rev. B **51**, 8164 (1995).
[4] A. K. Jonscher, Nature (London) **267**, 673 (1977).
[5] K. L. Ngai and S. W. Martin, Phys. Rev. B **40**, 10 550 (1989).
[6] C. A. Angell, Chem. Rev. **90**, 523 (1990).
[7] H. Kahnt, Ber. Bunsenges. Phys. Chem. **95**, 1021 (1991).
[8] C. T. Moynihan, J. Non-Cryst. Solids **172–174**, 1395 (1994).
[9] H. Jain and X. Lu, J. Am. Ceram. Soc. **80**, 517 (1997).
[10] D. L. Sidebottom, Phys. Rev. Lett. **82**, 3653 (1999).
[11] B. Roling and C. Martiny, Phys. Rev. Lett. **85**, 1274 (2000).
[12] S. R. Elliott and A. P. Owens, Ber. Bunsenges. Phys. Chem. **95**, 987 (1991).
[13] A. Bunde, M. D. Ingram, and P. Maass, J. Non-Cryst. Solids **172–174**, 1222 (1994).
[14] D. Knöedler, P. Pendzig, and W. Dieterich, Solid State Ionics **86–88**, 29 (1996).
[15] K. Y. Tsang and K. L. Ngai, Phys. Rev. E **56**, R17 (1997).
[16] K. Funke and D. Wilmer, in *Solid State Ionics V*, edited by G.-A. Nazri, C. Julien, and A. Rougier, Mater. Res. Soc. Symp. Proc. Proceedings No. 548 (Materials Research Society, Pittsburgh, 1999), p. 403.
[17] P. Maass, J. Non-Cryst. Solids **255**, 35 (1999).
[18] T. B. Schroder and J. C. Dyre, Phys. Rev. Lett. **84**, 310 (2000).
[19] J. C. Dyre, Phys. Rev. B **49**, 11 709 (1994).
[20] I. Svare, F. Borsa, D. R. Torgeson, and S. W. Martin, J. Non-Cryst. Solids **172–174**, 1300 (1994).
[21] S. Sen, A. M. George, and J. F. Stebbins, J. Non-Cryst. Solids **197**, 53 (1996).
[22] S. D. Baranovskii and H. Cordes, J. Chem. Phys. **111**, 7546 (1999).
[23] B. Roling, Phys. Rev. B **61**, 5993 (2000).
[24] K. Funke, B. Roling, and M. Lange, Solid State Ionics **105**, 195 (1998).
[25] D. Knödler, P. Pendzig, and W. Dieterich, Solid State Ionics **70**, 356 (1994).
[26] B. Roling, C. Martiny, and K. Funke, J. Non-Cryst. Solids **249**, 201 (1999).
[27] H. Jain, E. I. Kamitsos, Y. D. Yiannopoulos, G. D. Chryssikos, W. C. Huang, R. Küchler, and O. Kanert, J. Non-Cryst. Solids **203**, 320 (1996).
[28] W. C. Huang, H. Jain, and M. A. Marcus, J. Non-Cryst. Solids **180**, 40 (1994).
[29] W. C. Huang and H. Jain, J. Non-Cryst. Solids **188**, 254 (1995).
[30] A. D. Cox and P. W. McMillian, J. Non-Cryst. Solids **44**, 257 (1981).
[31] S. Sakka and K. Kamiya, J. Non-Cryst. Solids **49**, 103 (1982).
[32] P. J. Bray, J. Non-Cryst. Solids **95/96**, 45 (1989).
[33] J. W. Zwanziger, R. E. Youngman, and S. L. Tagg, J. Non-Cryst. Solids **192&193**, 157 (1995).
[34] H. E. Taylor, J. Soc. Glass Technol. **43**, 124T (1959).
[35] J. O. Isard, J. Non-Cryst. Solids **4**, 357 (1970).
[36] B. Roling, A. Happe, K. Funke, and M. D. Ingram, Phys. Rev. Lett. **78**, 2160 (1997).
[37] B. Roling, Solid State Ionics **105**, 185 (1998).
[38] F. Kohler, *The Liquid State* (Verlag Chemie, Weinheim, 1972), p. 163.
[39] D. A. McQuarrie, *Statistical Mechanics* (Harper Collins, New York, 1976), p. 582.
[40] J. E. Kelly III, J. F. Cordaro, and M. Tomozawa, J. Non-Cryst. Solids **41**, 47 (1980).
[41] M. Tomozawa and J. E. Kelly III, J. Non-Cryst. Solids **51**, 345 (1982).
[42] H. Kahnt, J. Non-Cryst. Solids **203**, 225 (1996).
[43] M. P. Thomas and N. L. Peterson, Solid State Ionics **14**, 297 (1984).
[44] R. W. Heckman, J. A. Ringlien, and E. L. Williams, Phys. Chem. Glasses **8**, 145 (1967).
[45] R. Terai and R. Hayami, J. Non-Cryst. Solids **18**, 217 (1975).
[46] H. Kahnt, Ch. Kaps, and J. Offermann, Solid State Ionics **31**, 215 (1988).
[47] Y. Haven and B. Verkerk, Phys. Chem. Glasses **6**, 38 (1965).
[48] Y. Kawamoto and M. Nishida, Phys. Chem. Glasses **18**, 19 (1977).
[49] J. M. Hyde and M. Tomozawa, J. Non-Cryst. Solids **109**, 18 (1989).
[50] P. A. V. Johnson, A. W. Wright, and R. N. Sinclair, J. Non-Cryst. Solids **50**, 281 (1982).
[51] W. L. Konijnendijk and J. M. Stevels, J. Non-Cryst. Solids **20**, 193 (1976).
[52] G. E. Jellison, Jr. and P. J. Bray, J. Non-Cryst. Solids **29**, 187 (1978).
[53] W. Vogel, *Glaschemie* (Springer-Verlag, Berlin, 1992).
[54] R. Zallen, *The Physics of Amorphous Solids* (Wiley, New York, 1983).
[55] R. H. Doremus, *Glass Science* (Wiley, New York, 1973).